Immobilization of β-glucosidase onto Magnetic Nanoparticles and Evaluation of the Enzymatic Properties

Ying Zhou,[a] Siyi Pan,[a,*] Xuetuan Wei,[b] Lufeng Wang,[a] and Yanlong Liu [a]

This paper reports on a novel and efficient β-glucosidase immobilization method using magnetic Fe_3O_4 nanoparticles as a carrier. Based on response surface methodology, the optimal immobilization conditions obtained were: glutaraldehyde (GA) concentration, 0.20%; enzyme concentration, 50.25 μg/mL; cross-linking time, 2.21 h; and the maximum activity recovery reached 89.35%. The magnetic immobilized enzyme was characterized by Fourier transform infrared spectroscopy (FTIR), transmission electron microscope (TEM), and vibrating sample magnetometer (VSM). FTIR revealed that β-glucosidase was successfully immobilized on the magnetic nanoparticles. TEM showed that enzyme-magnetic nanoparticles possessed nano-scale size distribution. VSM confirmed that the enzyme-magnetic nanoparticles were superparamagnetic. The properties of the immobilized β-glucosidase were improved, and the immobilized β-glucosidase exhibited wider pH and temperature ranges of activation, higher accessibility of the substrate, better thermal stability, and better storage stability than that of the free enzyme. The enzyme-magnetic nanoparticles could be separated magnetically for easy reuse. Immobilization of β-glucosidase onto the magnetic nanoparticles has the potential for industrial application.

Keywords: Magnetic nanoparticles; β-glucosidase; Immobilization; Response surface methodology; Characterization

Contact information: a: College of Food Science and Technology, Huazhong Agricultural University, Wuhan, Hubei 430070 China; b: Key Laboratory of Green Process and Engineering, Institute of Process Engineering, Chinese Academy of Sciences, Beijing 100190 China;
** Corresponding author: pansiyi@mail.hzau.edu.cn*

INTRODUCTION

Cellulose, the largest component of woody materials, is a renewable resource that has potential for large-scale production of biofuel. Traditional chemical processes for cellulose degradation usually involve high temperatures, high pressure, and strongly acidic and strongly alkaline conditions. Compared to these chemical methods, enzymatic hydrolysis methods involve lower energy consumption, milder reaction conditions, higher yields, and substrate specificity (Maeda *et al.* 2012; MartináAlonso 2013). β-glucosidase (EC 3.2.1.21) can hydrolyze various glycosides, and multiple potential applications have been developed in cellulose degradation (Gefen *et al.* 2012). However, free β-glucosidase has some limitations for industrial applications, such as a tedious recycle process and poor stability. Enzyme immobilization technology can overcome these drawbacks and therefore is a good choice for wider applications. β-glucosidase has been immobilized on various supports, while the activity recovery is still low, such as for

chitosan (25.1%), sol-gel beads (28%), sodium alginate (28.2%), Eupergit C (83%), and S-layer (37%) (Balogh *et al.* 2005; Fan *et al.* 2011; Mayer *et al.* 2010; O'Neill *et al.* 2002; Su *et al.* 2010; Tu *et al.* 2006), and thus the activity recovery needs to be further improved.

Due to the ease of separation and reuse, magnetic materials have been used as the immobilization carriers for enzyme. In the work of Dekker (1990), the β-glucosidase was immobilized onto two kinds of magnetite (polyethyleneimine-glutaraldehyde activated, and TiO_2-coated magnetite); it was found that low activity recovery and poor substrate accessibility limited its industrial application (Dekker 1990).

Compared to magnetite, nanoscale magnetic particles have much larger specific surface area, greatly improving the loading capacity and reducing the diffusion limitation. For this reason, magnetic nanoparticles have drawn increasing attention for immobilization processes. Magnetic nanoparticles have also been used for the immobilization of enzymes, such as enterokinase (Santana *et al.* 2012), α-amylase (Namdeo and Bajpai 2009; Talekar *et al.* 2012), and lipase (Cui *et al.* 2010). Furthermore, these enzymes immobilized onto magnetic nanoparticles showed high activity recovery and improved enzyme properties. Therefore, magnetic nanoparticles have the potential to improve immobilization activity recovery and enzyme properties. To the best of our knowledge, magnetic nanoparticles have never been used for β-glucosidase immobilization.

Superparamagnetic nanoparticles of 1 to 10 nm of particle size will not possess the internal magnetic field in the absence of an external magnetic field. Thus, collection and redispersion of superparamagnetic nanoparticles can be easily carried out by regulation of the external magnetic field. By contrast, ferromagnetic materials would exhibit very large internal magnetic fields in any case, and they would usually exist as a large aggregation. Therefore, superparamagnetic nanoparticles have been widely applied, with applications such as electrochemical sensors (Li *et al.* 2012), magnetic targeted drug delivery (Chen *et al.* 2012; Xu *et al.* 2010), removal of heavy metals (Wang *et al.* 2009), and embolotherapy (Chan *et al.* 2006; Chung *et al.* 2012). Herein, superparamagnetic nanoparticles were used as the support for immobilization of β-glucosidase. Superparamagnetic nanoparticles were synthesized by a co-precipitating method, and coated with sodium citrate. The immobilization conditions were optimized by response surface methodology to obtain the maximum activity recovery. Further, the enzyme-magnetic nanoparticles were characterized by transmission electron microscopy (TEM), Fourier transform infrared spectroscopy (FTIR), and a vibrating sample magnetometer (VSM). The properties of the immobilized β-glucosidase were further investigated.

EXPERIMENTAL

Materials

The β-glucosidase (2.18 U/mg) used in this study was bought from Sigma-Aldrich. 4-nitrophenyl-β-D-glucopyranoside (p-NPG) was purchased from Shanghai Source Leaves Biological Technology. Glutaraldehyde (25% in v/v), $FeCl_3$•$6H_2O$, $FeCl_2$•$4H_2O$, and other reagents were obtained from Sinopharm Chemical Reagent.

Preparation of Magnetic Fe_3O_4 Nanoparticles

The magnetic Fe_3O_4 nanoparticles were synthesized by the co-precipitating method with minor modification (Pan *et al.* 2009). $FeCl_3 \cdot 6H_2O$ (4.335 mmol) and

$FeCl_2 \cdot 4H_2O$ (2.17 mmol) were dissolved in 50 mL distilled water in a 250-mL, three-neck flask. Thereafter, the reaction temperature was raised to 85 °C and the above solution was stirred at 85 °C for 30 min with N_2 as the protective gas. Subsequently, $NH_3 \cdot H_2O$ (25 mL) was added to the solution with vigorous stirring, and sodium citrate (0.13 mmol) was immediately added when the color of the solution changed to black, and the solution was stirred at 85 °C for another 30 min. Finally, the magnetic Fe_3O_4 nanoparticles were obtained after magnetic separation and washed with distilled water to neutral pH.

Immobilization of β-Glucosidase on Magnetic Fe_3O_4 Nanoparticles

First, 100 μL magnetic Fe_3O_4 nanoparticles (300 mg/mL) were dispersed in 900 μL of 100 mmol phosphate–citric acid buffer (pH 5.0) containing 0.2% (v/v) glutaraldehyde by ultrasonic dispersion for 20 min at room temperature. Then 1 mL of β-glucosidase solution (0.05 mg/mL) was added to the mixture and incubated at 25 °C with shaking (150 rpm). Magnetic Fe_3O_4 nanoparticles with β-glucosidase were collected magnetically and washed thrice with 100 mmol phosphate–citric acid buffer (pH 5.0). The activity recovery of the immobilized β-glucosidase was calculated as,

$$\text{Activity recovery (\%)} = [\, A_{immob} / A_{init} \,] \times 100\% \quad (1)$$

where A_{immob} is the immobilized enzyme activity and A_{init} is the initial (free) enzyme activity.

Determination of β-Glucosidase Activity

β-Glucosidase activity was determined by adding 100 of μL enzyme solution to 900 μL of 100 mM phosphate–citric acid buffer (pH 5.0) containing 10 mM p-NPG. The reaction mixtures were incubated at 50 °C for 15 min and stopped by adding 1 mL of 2 M Na_2CO_3. Subsequently, the released p-nitrophenol was measured at $\lambda = 400$ nm. One unit of β-glucosidase activity was defined as the amount of enzyme to release 1 μmol of p-nitrophenol per minute.

Experimental Design and Statistical Analyses

Based on the results of the single-factor experiments (data not shown), a 3-level, 3-factor Box–Behnken design requiring 15 experiments was performed for optimization of enzyme immobilization to acquire the maximum activity recovery. Table 1 represents the levels of each factor. The experimental data in terms of activity recovery are recorded in Table 2. Experimental design and the statistical analysis of the results were performed by Minitab Statistical Software. All experiments were repeated at least three times.

Table 1. Levels of Design Variables and Coding of Levels

Design Variable	Coding of Levels		
	−1	0	1
GA concentration (%)	0.1	0.2	0.3
Enzyme concentration (mg/ml)	0.025	0.05	0.075
Cross-linking time (h)	1	2	3

Characterization of Magnetic and Enzyme-magnetic Nanoparticles

The FTIR spectra of the magnetic and enzyme-magnetic nanoparticles were recorded on a VERTEX 70 spectrometer (Bruker, Germany) operating from 4000 to 400 cm^{-1}. The size and morphology of magnetic and enzyme-magnetic nanoparticles were observed by TEM (Hitachi H-700FA, Japan). The magnetic properties of the magnetic and enzyme-magnetic nanoparticles were evaluated using a VSM instrument (LakeShore 7404, USA) under ambient temperature.

Table 2. Response Surface Results for the Box–Behnken Design of Factors and Activity Recovery of Different Parameters

Run	Coded Levels			Actual Levels			Activity Recovery (%)
	A	B	C	A	B	C	
1	−1	0	1	0.1	0.05	3	75.75
2	1	0	−1	0.3	0.05	1	79.12
3	1	1	0	0.3	0.075	2	45.51
4	−1	−1	0	0.1	0.025	2	44.75
5	1	0	1	0.3	0.05	3	74.82
6	0	1	1	0.2	0.075	3	58.90
7	0	0	0	0.2	0.05	2	89.10
8	−1	0	−1	0.1	0.05	1	76.44
9	0	−1	−1	0.2	0.025	1	60.13
10	0	1	−1	0.2	0.075	1	60.21
11	0	0	0	0.2	0.05	2	89.54
12	0	−1	1	0.2	0.025	3	57.22
13	1	−1	0	0.3	0.025	2	58.58
14	0	0	0	0.2	0.05	2	89.03
15	−1	1	0	0.1	0.075	2	59.02

A: GA concentration (%)
B: Enzyme concentration (mg/mL)
C: The cross-linking time (h)

Evaluation of Enzyme Properties of the Immobilized β-glucosidase

The optimum reaction pH of free and immobilized β-glucosidase was measured in the pH range between 3.0 and 7.0, and the optimum temperature was measured at diverse temperatures (30 to 80 °C) in a water bath.

The thermal stability was also evaluated by maintaining the enzyme at different temperatures (from 30 to 80 °C) for 1 h. Kinetic parameters of the Michaelis constant (Km) of free and immobilized β-glucosidase was investigated by measuring the enzyme activity with p-NPG (0.5 to 20 mM) at constant temperature and pH, calculated by the Lineweaver–Burk plot (Lineweaver and Burk 1934).

The storage stability was evaluated by storing in 100 mM Na_2HPO_4-$C_6H_8O_7$ buffer (pH 5.0) at 4 °C for 6 weeks. For a reusability assessment, immobilized β-glucosidase was recovered with magnetic separation after determination of β-glucosidase activity, and the procedure was repeated under the same conditions for every batch.

RESULTS AND DISCUSSION

Optimization of Immobilization Conditions

Response Surface Methodology (RSM) is a statistical and graphical technique for developing, improving, and optimizing processes, which can overcome the following disadvantages: the classical one-factor-one-time method in a time-consuming process; unrealistic number of experiments; and difficulties in determination of optimal conditions (Bouaid *et al.* 2009). Box–Behnken designs are an especially efficient response surface method for obtaining mathematical models (Ebrahimi *et al.* 2010).

The β-glucosidase immobilized onto the citrate-modified Fe_3O_4 nanoparticles using glutaraldehyde as the cross-linking agent is schematically illustrated in Fig. 1. Based on analysis of the single-factor experiments (data not shown), response surface methodology was used to further optimize the three factors for the maximum activity recovery of immobilized β-glucosidase. A Box–Behnken design of three centre points with 15 experiments was performed to better evaluate the effect of each factor and its complex interactions. By applying regression analysis (Table 3), a quadratic polynomial equation was established to explain the relationship between the activity recovery and the independent variables as follows,

$$Y = 89.2233 + 0.4018 \times A + 0.3701 \times B - 1.1495 \times C - 9.9196 \times A^2 - 27.3393 \times B^2 - 2.7688 \times C^2 - 6.8343 \times A \times B - 0.9028 \times A \times C + 0.2593 \times B \times C \quad (2)$$

where Y, A, B, and C represented the activity recovery, GA concentration, enzyme concentration, and cross-linking time, respectively. Regression analysis (Table 3) showed a coefficient of determination (R^2) value to be 0.9998, meaning that the model as fitted explained 99.98% of the variability in activity recovery.

Table 3. Estimated Regression Coefficients and R-squared Values of the Box–Behnken Design

Term	Coefficient	SE Coefficient	T Ratio	P Value
Constant	89.2233	0.1877	475.318	0.000**
A: GA concentration (%)	0.4018	0.115	2.256	0.074
B: enzyme concentration (mg/mL)	0.3701	0.115	3.22	0.023*
C: cross-linking time (h)	−1.1495	0.115	−10	0.000**
A*A	−9.9196	0.1692	−58.626	0.000**
B*B	−27.3393	0.1692	−161.578	0.000**
C*C	−2.7688	0.1692	−16.364	0.000**
A*B	−6.8343	0.1626	−42.04	0.000**
A*C	−0.9028	0.1626	−5.554	0.003**
B*C	0.2593	0.1626	2.472	0.056
R^2 = 0.9998	R^2 (adj) = 0.9995	R^2 (pred) = 0.9980		
* Significant at 5% level ** Significant at 1% level				

The high adjusted R^2 value (0.9995) revealed the high significance of this model. According to the regression analysis (Table 3), the regression coefficients of the linear terms (C), the quadratic terms (A^2, B^2, C^2), and the interaction term (A×B) were all found to be significant at the 1% level, and the regression coefficients of the linear terms (B) and the interaction term (A×C) were both found to be significant at the 5% level, indicating that the above coefficients have remarkable influence on the immobilization of β-glucosidase.

Based on the summary of variance (ANOVA) for the model of activity recovery (Table 4), the computed F ratio of 3352.72 (P value of 0.000) illustrated that the model was extremely significant. Furthermore, the lack of fit F ratio was 1.58 and the P value was 0.41, both implying that the experimental data procured fitted properly with this model.

Table 4. Analysis of Variance (ANOVA) for the Results of the Box–Behnken Design

Source	DF	Seq SS	Adj SS	Adj MS	F Ratio	P Value
Regression	9	3189.69	3189.69	354.41	3352.72	0.000**
Linear	3	12.2	12.2	4.068	38.48	0.001**
Square	3	2986.75	2986.75	995.584	9418.23	0.000**
Interaction	3	190.73	190.73	63.578	601.45	0.000**
Residual error	5	0.53	0.53	0.106		
Lack of fit	3	0.37	0.37	0.124	1.58	0.41
Pure error	2	0.16	0.16	0.078		
Total	14	3190.22				
** Significant at 1% level						

The planned series of response surface and contour plots (Fig. 2) were utilized for better understanding of the interactions among the three variables (GA concentration, enzyme concentration, and cross-linking time). Corresponding to the optimum levels of all variables, the maximum activity recovery was determined and also indicated the same result. Optimal conditions of GA concentration, enzyme concentration, and cross-linking time were 0.20%, 50.25 μg/mL, and 2.21 h, respectively, resulting in the maximum activity recovery (89.35%). Experimental verification of the predicted result was performed under the optimal levels, and the experimental value was 90.46%, which was in close agreement with the predicted value by the model based on the Box–Behnken design (89.35%). Consequently, optimization of enzyme immobilization using RSM exhibited the maximal activity recovery of immobilized β-glucosidase using a 3-level, 3-factor Box–Behnken design. This model could be considered quite accurate and reliable for predicting the activity recovery for immobilized β-glucosidase. The activity recovery of several reported supports for β-glucosidase immobilization, such as magnetite (15-27%), chitosan (25.1%), sol-gel beads (28%), sodium alginate (28.2%), Eupergit C (30%), S-layer (37%), and agarose matrix, functionalized with distinct reactive groups (80%), were still low (Balogh *et al.* 2005; Fan *et al.* 2011; O'Neill *et al.* 2002; Palmeri and Spagna 2007; Su *et al.* 2010; Tu *et al.* 2006). Therefore, the activity recovery of the present method was much higher than other methods, and magnetic Fe_3O_4 nanoparticles showed obvious advantages for enhancement of the activity recovery of immobilized β-glucosidase.

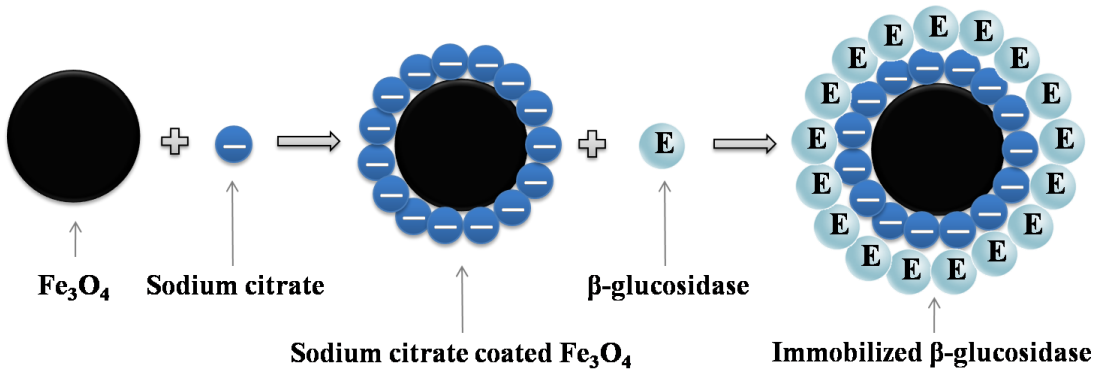

Fig. 1. Schematic illustration of the fabrication strategy for β-glucosidase immobilized on the magnetic nanoparticles

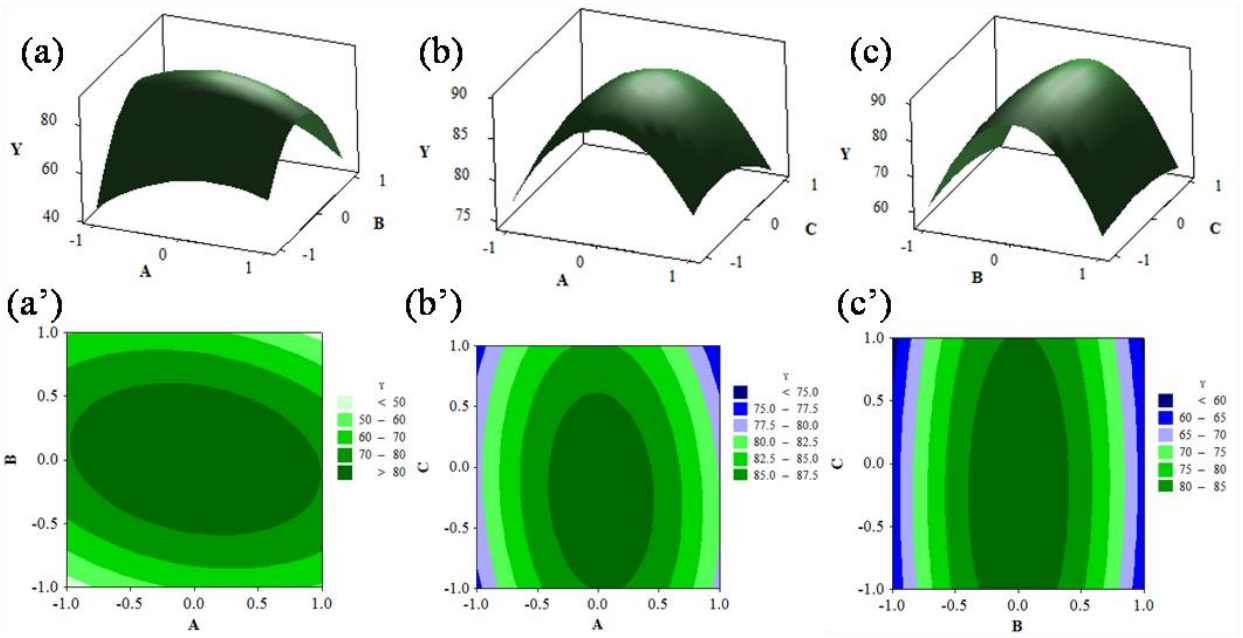

Fig. 2. Diagrams (a, a', to c, c') showing the response surface plots and contour plots for the three independent variables (dependent variable = Y: activity recovery; A: GA concentration; B: enzyme concentration; C: cross-linking time)

Characterization of Magnetic and Enzyme-magnetic Nanoparticles

FTIR spectral analysis

As shown in Fig. 3, FTIR spectra of both magnetic and enzyme-magnetic nanoparticles showed absorption peaks near 581 cm^{-1}, corresponding to the stretching vibration for the Fe–O bond, revealing the existence of Fe_3O_4. The FTIR spectra of enzyme-magnetic nanoparticles showed an absorption peak near 1543 cm^{-1} (–N–H stretch vibrations), which can only be assigned to the β-glucosidase in all added materials, confirming the existence of β-glucosidase onto the magnetic nanoparticles. Accordingly, the characteristic peak of carbonyl stretch of β-glucosidase is also shown at 1656 cm^{-1} in the FTIR spectra.

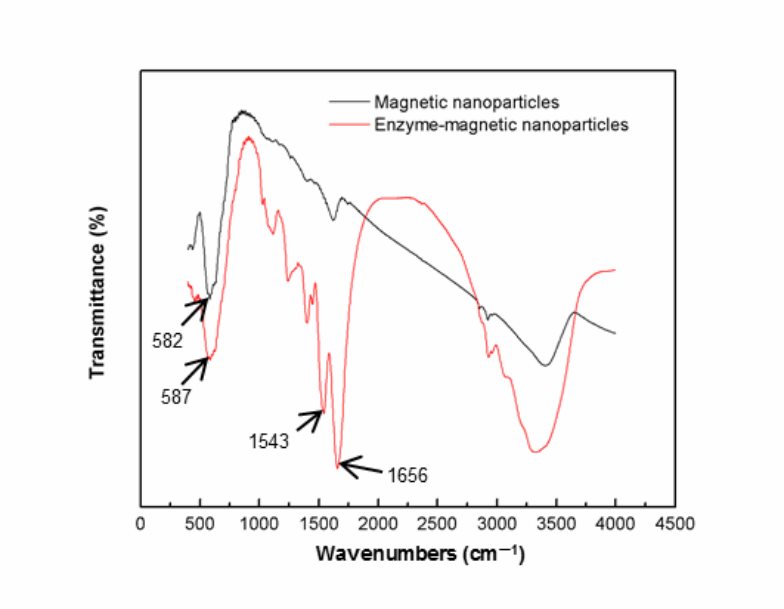

Fig. 3. FTIR spectra of magnetic and enzyme-magnetic nanoparticles

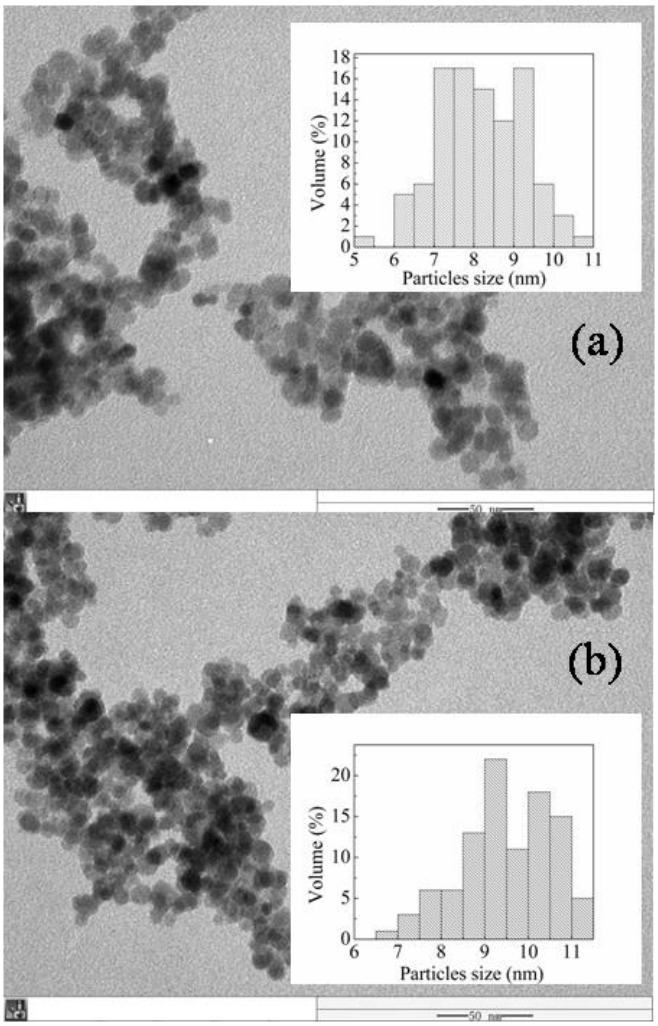

Fig. 4. Typical TEM image and particles size distribution of magnetic (a) and enzyme-magnetic nanoparticles (b)

TEM analysis

From the typical TEM image (Fig. 4), the magnetic nanoparticles showed circular morphology with an average particle size of 8.13±1.07 nm, and the enzyme-magnetic nanoparticles showed similar morphology and mean particle size (9.47±1.04 nm). Furthermore, both the magnetic and enzyme-magnetic nanoparticles showed good dispersibility, indicating that immobilization did not affect the stability of magnetic nanoparticles.

Magnetic properties analysis

Figure 5 shows the magnetic hysteresis loops of the magnetic and enzyme-magnetic nanoparticles.

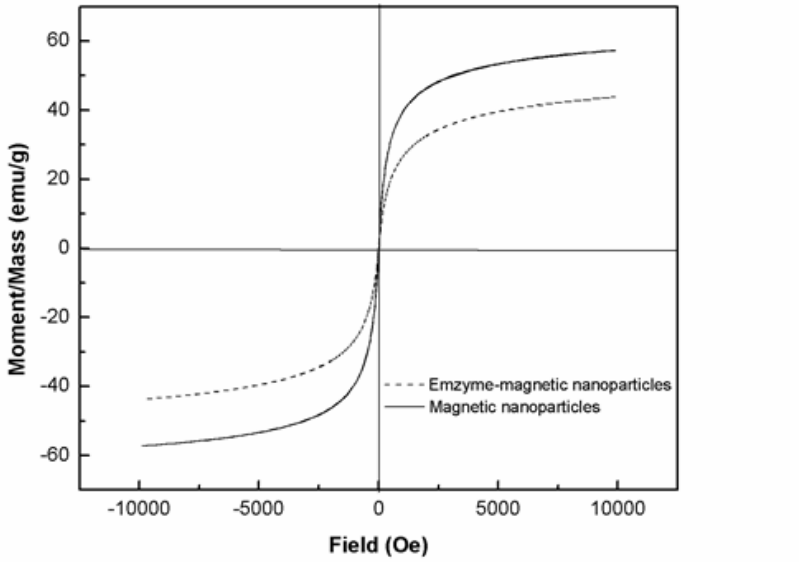

Fig. 5. Magnetic hysteresis loops of magnetic and enzyme-magnetic nanoparticles

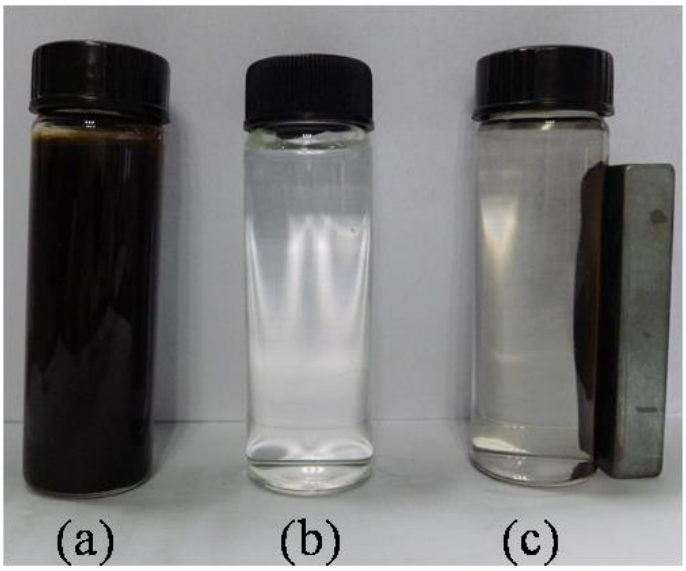

Fig. 6. Photograph of nanoparticles' stable dispersion: (a) magnetic nanoparticles; (b) free enzyme; (c) enzyme-magnetic nanoparticles under an external magnetic field

Both sets of results showed no hysteresis without remanence and coercivity, indicating that both the magnetic and enzyme-magnetic nanoparticles were superparamagnetic. Compared with the magnetization (Ms) of magnetic nanoparticles (57.3 emu/g), the Ms of enzyme-magnetic nanoparticles (43.8 emu/g) was slightly lower, which was attributed to the tight attachment of β-glucosidase onto the surface. In addition, Fig. 6 shows that the resultant enzyme-magnetic nanoparticles could be easily separated by use of an external magnet, which contributed to separation and reuse of the immobilized enzyme.

Properties of the Immobilized β-glucosidase

Optimum pH and temperature

As shown in Fig. 7a, the optimal pH was 5.0 for the free β-glucosidase and 4.0 for the immobilized β-glucosidase. At low pH the enzyme activity was increased greatly after immobilization, such that the immobilized β-glucosidase had a wider pH range of effectiveness.

As shown in Fig. 7b, the optimal temperature of free and immobilized β-glucosidase was 60 °C and 70 °C, respectively. The shift toward high temperature after immobilization might be attributed to the multipoint chelate interaction (Kara *et al.* 2005; Sari *et al.* 2006).

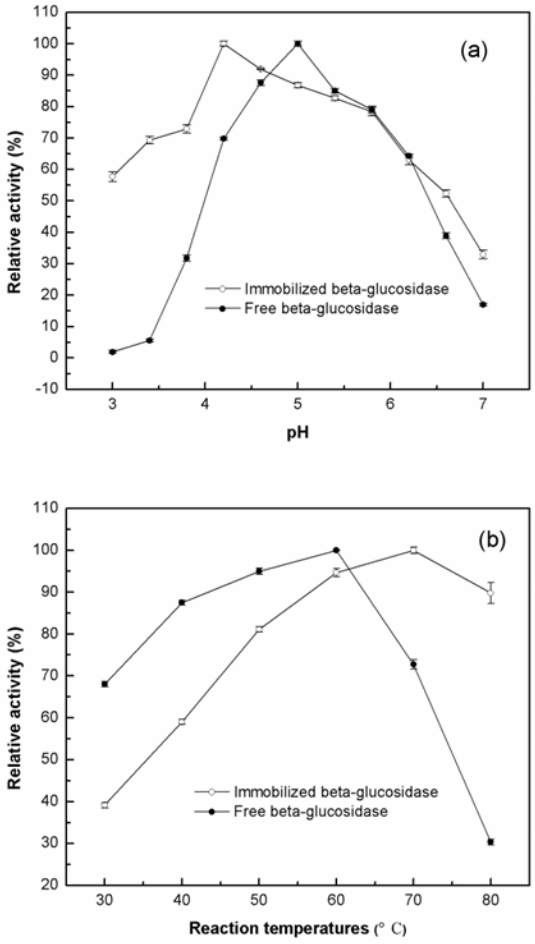

Fig. 7. Effect of pH (a) and temperature (b) on the activity of free and immobilized β-glucosidase

Kinetic parameters

The Michaelis constant (K_m) of the free and immobilized β-glucosidase was calculated according to the Lineweaver–Burk plot shown in Fig. 8. The K_m value of immobilized β-glucosidase (1.77 mmol/L) was lower than that of the free enzyme (3.12 mmol/L), suggesting that the immobilized β-glucosidase possessed higher accessibility to the substrate than the free enzyme. By contrast, magnetite as the carrier has been shown to increase the K_m value (Dekker 1990). These results indicated that magnetic nanoparticles are preferable carriers for enhancement of the substrate accessibility. The decrease in K_m of the immobilized β-glucosidase has also been reported for other supports (Fan *et al.* 2011; Su *et al.* 2010).

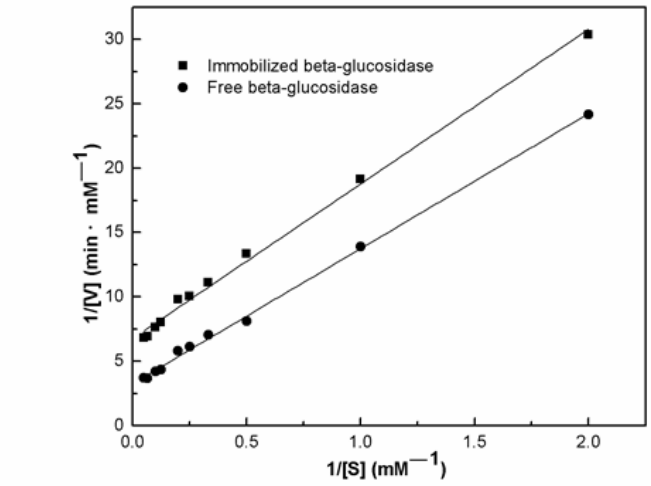

Fig. 8. Lineweaver–Burk double reciprocal plots of free and immobilized β-glucosidase

Thermal stability

Under high temperature conditions (50 to 80 °C), immobilized β-glucosidase showed higher enzyme activity than that of free β-glucosidase (Fig. 9).

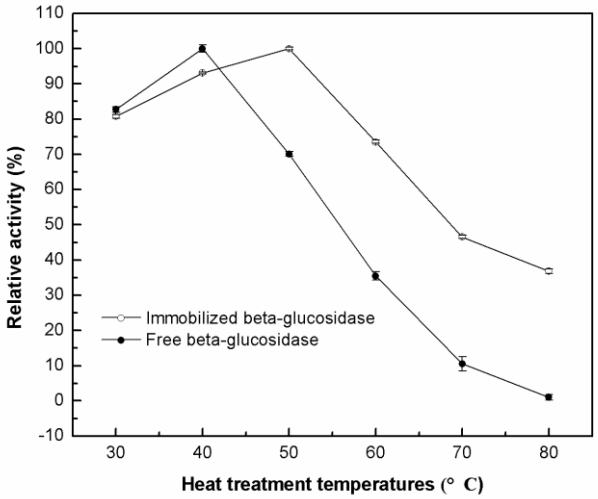

Fig. 9. Thermal stability of the free and immobilized β-glucosidase

Moreover, the immobilized β-glucosidase was found to possess 75% of its original activity, whereas the free enzyme remained at 35% at 60 °C. It was obvious that the immobilized β-glucosidase was more stable than the free β-glucosidase due to the increased rigidity of the enzyme after immobilization (Chiou and Wu 2004; Jung *et al.* 2011; Yodoya *et al.* 2003).

Storage stability and reusability

As shown in Fig. 10a, the immobilized β-glucosidase retained about 73% of its initial activity after 6 weeks of storage, whereas the free β-glucosidase lost more than 80% of its initial activity. These results indicated that the immobilization with magnetic nanoparticles improved the stability of β-glucosidase, and similar results have been reported for other immobilization methods (Fan *et al.* 2011; González-Pombo *et al.* 2011; Su *et al.* 2010).

The reusability of the immobilized β-glucosidase is an important characteristic for its potential industrial applications. As shown in Fig. 10b, the immobilized β-glucosidase maintained about 86% of its original activity after 10 consecutive operations. The activity loss of immobilized enzyme probably could be due to the conformational changes and the leakage from the carriers.

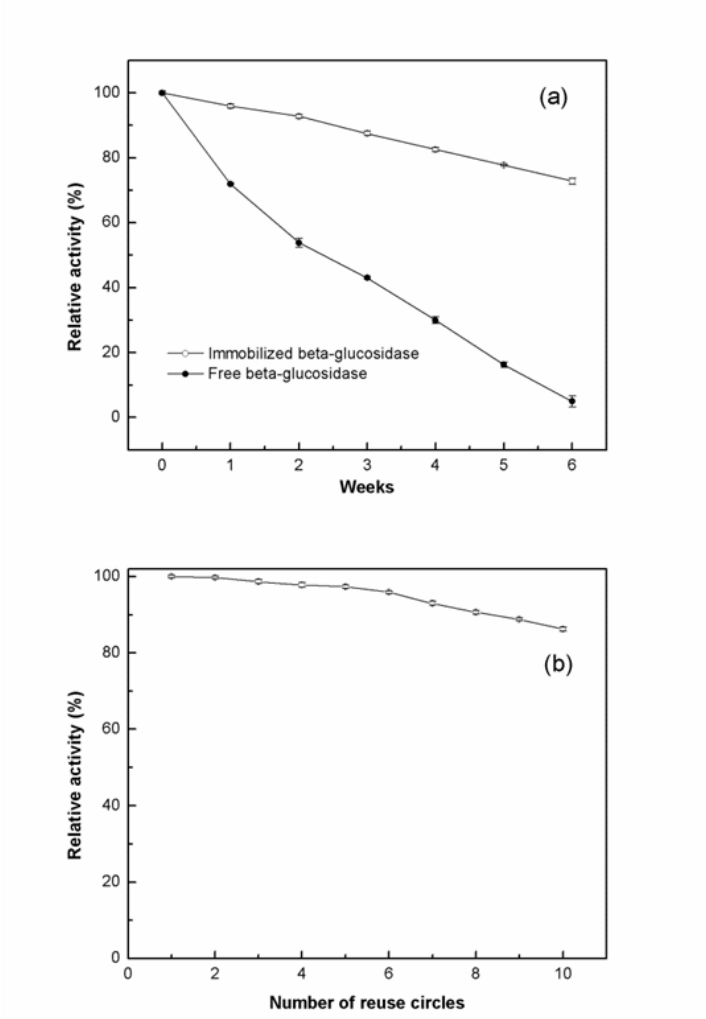

Fig. 10. Storage stability (a) and reusability (b) of the free and immobilized β-glucosidase

CONCLUSIONS

1. β-glucosidase was immobilized onto the citrate-modified Fe_3O_4 nanoparticles *via* a glutaraldehyde cross-linking reaction, and the optimal immobilization conditions and a high activity recovery were obtained using RSM.
2. FTIR and TEM analyses indicated that β-glucosidase immobilized onto magnetic nanoparticles presented good nano-scale dispersibility.
3. Importantly, the magnetic immobilization improved the enzyme properties of β-glucosidase. The reaction pH and temperature range were broadened, and the accessibility of the substrate, thermal stability, and storage stability were enhanced.
4. Enzyme-magnetic nanoparticles were superparamagnetic, and the immobilized β-glucosidase could be separated easily for constant application.

REFERENCES CITED

Balogh, T., Tóth, Á. and Kosáry, J. (2005). "S-layer, a new support for enzyme immobilization," *Acta Alimentaria* 34, 203-208.

Bouaid, A., Martinez, M. and Aracil, J. (2009). "Production of biodiesel from bioethanol and Brassica carinata oil: Oxidation stability study," *Bioresour. Technol.* 100, 2234-2239.

Chan, H., Do, Y.Y., Huang, P., Chien, P., Chan, T., Liu, R., Huang, C., Yang, S. and Horng, H. (2006). "Preparation and properties of bio-compatible magnetic Fe_3O_4 nanoparticles," *J. Magn. Magn. Mater.* 304, e415-e417.

Chen, W., Cao, Y., Liu, M., Zhao, Q., Huang, J., Zhang, H., Deng, Z., Dai, J., Williams, D.F. and Zhang, Z. (2012). "Rotavirus capsid surface protein VP4-coated Fe_3O_4 nanoparticles as a theranostic platform for cellular imaging and drug delivery," *Biomaterials* 33, 7895-7902.

Chiou, S.H. and Wu, W.T. (2004). "Immobilization of *Candida rugosa* lipase on chitosan with activation of the hydroxyl groups," *Biomaterials* 25, 197-204.

Chung, E. Y., Kim, H. M., Lee, G. H., Kwak, B. K., Jung, J. S., Kuh, H. J. and Lee, J. (2012). "Design of deformable chitosan microspheres loaded with superparamagnetic iron oxide nanoparticles for embolotherapy detectable by magnetic resonance imaging," *Carbohydr. Polym.* 90, 1725-1731.

Cui, Y., Li, Y., Yang, Y., Liu, X., Lei, L., Zhou, L. and Pan, F. (2010). "Facile synthesis of amino-silane modified superparamagnetic Fe_3O_4 nanoparticles and application for lipase immobilization," *J. Biotechnol.* 150, 171-174.

Dekker, R. F. (1990). "Application of a magnetic immobilizedβ-glucosidase in the enzymatic saccharification of steam-exploded lignocellulosic residues," *Appl. Biochem. Biotechnol.* 23, 25-39.

Ebrahimi, B., Shojaosadati, S., Ranaie, S. and Mousavi, S. (2010). "Optimization and evaluation of acetylcholine esterase immobilization on ceramic packing using response surface methodology," *Process Biochem.* 45, 81-87.

Fan, G., Xu, Y., Zhang, X., Lei, S., Yang, S. and Pan, S. (2011). "Characteristics of immobilised β - glucosidase and its effect on bound volatile compounds in orange juice," *International Journal of Food Science & Technology* 46, 2312-2320.

Gefen, G., Anbar, M., Morag, E., Lamed, R. and Bayer, E. A. (2012). "Enhanced cellulose degradation by targeted integration of a cohesin-fused β-glucosidase into the Clostridium thermocellum cellulosome," *Proceedings of the National Academy of Sciences* 109, 10298-10303.

González-Pombo, P., Fariña, L., Carrau, F., Batista-Viera, F. and Brena, B. M. (2011). "A novel extracellular beta-glucosidase from Issatchenkia terricola: Isolation, immobilization and application for aroma enhancement of white Muscat wine," *Process Biochem.* 46, 385-389.

Jung, Y. R., Shin, H. Y., Song, Y. S., Kim, S. B. and Kim, S. W. (2011). "Enhancement of immobilized enzyme activity by pretreatment of β-glucosidase with cellobiose and glucose," *J. Ind. Eng. Chem.* 18, 702-706.

Kara, A., Osman, B., Yavuz, H., Beşirli, N. and Denizli, A. (2005). "Immobilization of α-amylase on Cu^{2+} chelated poly (ethylene glycol dimethacrylate-*n*-vinyl imidazole) matrix via adsorption," *React. Funct. Polym.* 62, 61-68.

Li, X., He, G., Han, Y., Xue, Q., Wu, X. and Yang, S. (2012). "Magnetic titania-silica composite-Polypyrrole core-shell spheres and their high sensitivity toward hydrogen peroxide as electrochemical sensor," *J. Colloid Interface Sci.* 387, 39-46.

Lineweaver, H. and Burk, D. (1934). "The determination of enzyme dissociation constants," *JACS* 56, 658-666.

Maeda, R. N., Barcelos, C. A., Anna, L. M. M. S. and Pereira, N. (2012). "Cellulase production by *penicillium funiculosum* and its application in the hydrolysis of sugar cane bagasse for second generation ethanol production by fed batch operation," *J. Biotechnol.* 163, 38-44.

MartináAlonso, D. (2013). "Integrated conversion of hemicellulose and cellulose from lignocellulosic biomass," *Energy Environ. Sci.* 6, 76-80.

Mayer, J., Kranz, B. and Fischer, L. (2010). "Continuous production of lactulose by immobilized thermostable β-glycosidase from *Pyrococcus furiosus*," *J. Biotechnol.* 145, 387-393.

Namdeo, M. and Bajpai, S. (2009). "Immobilization of α-amylase onto cellulose-coated magnetite (CCM) nanoparticles and preliminary starch degradation study," *J. Mol. Catal. B: Enzym.* 59, 134-139.

O'Neill, H., Angley, C. V., Hemery, I., Evans, B. R., Dai, S. and Woodward, J. (2002). "Properties of carbohydrate-metabolizing enzymes immobilized in sol-gel beads: stabilization of invertase and β;-glucosidase by Blue Dextran**," *Biotechnol. Lett* 24, 783-790.

Palmeri, R. and Spagna, G. (2007). "β-Glucosidase in cellular and acellular form for winemaking application," *Enzyme Microb. Technol.* 40, 382-389.

Pan, C., Hu, B., Li, W., Sun, Y., Ye, H. and Zeng, X. (2009). "Novel and efficient method for immobilization and stabilization of β-d-galactosidase by covalent attachment onto magnetic Fe_3O_4–chitosan nanoparticles," *J. Mol. Catal. B: Enzym.* 61, 208-215.

Santana, S. D. F., Pina, A. S. and Roque, A. C. A. (2012). "Immobilization of enterokinase on magnetic supports for the cleavage of fusion proteins," *J. Biotechnol.* 161, 378-382.

Sari, M., Akgöl, S., Karatas, M. and Denizli, A. (2006). "Reversible immobilization of catalase by metal chelate affinity interaction on magnetic beads," *Industrial & engineering chemistry research* 45, 3036-3043.

Su, E., Xia, T., Gao, L., Dai, Q. and Zhang, Z. (2010). "Immobilization of β-glucosidase and its aroma-increasing effect on tea beverage," *Food Bioprod. Process.* 88, 83-89.

Talekar, S., Ghodake, V., Ghotage, T., Rathod, P., Deshmukh, P., Nadar, S., Mulla, M. and Ladole, M. (2012). "Novel magnetic cross-linked enzyme aggregates (magnetic CLEAs) of alpha amylase," *Bioresour. Technol.* 123, 542-547.

Tu, M., Zhang, X., Kurabi, A., Gilkes, N., Mabee, W. and Saddler, J. (2006). "Immobilization of β-glucosidase on Eupergit C for lignocellulose hydrolysis," *Biotechnol. Lett* 28, 151-156.

Wang, X., Zhao, C., Zhao, P., Dou, P., Ding, Y. and Xu, P. (2009). "Gellan gel beads containing magnetic nanoparticles: An effective biosorbent for the removal of heavy metals from aqueous system," *Bioresour. Technol.* 100, 2301-2304.

Xu, P., Guo, F., Huang, J., Zhou, S., Wang, D., Yu, J. and Chen, J. (2010). "Alginate-based ferrofluid and magnetic microsphere thereof," *Int. J. Biol. Macromol.* 47, 654-660.

Yodoya, S., Takagi, T., Kurotani, M., Hayashi, T., Furuta, M. and Oka, M. (2003). "Immobilization of bromelain onto porous copoly (γ-methyl-L-glutamate/L-leucine) beads," *Eur. Polym. J.* 39, 173-180.

Article submitted: January 18, 2013; Peer review completed: March 26, 2013; Revised version received and accepted: April 2, 2013; Published: April 9, 2013.